Quantitative Assessment of Chronic Exposure to Cigarette Smoke in Mouse Lungs by Hyperpolarized Gas MRI

Y. Xin[1], K. Emami[1], S. J. Kadlecek[1], P. Mongkolwisetwara[1], N. N. Kuzma[1], H. Profka[1], Y. Xu[1], H. Hamedani[1], B. M. Pullinger[1], R. K. Ghosh[1], J. N. Rajaei[1], S. Pickup[1], M. Ishii[2], and R. R. Rizi[1]

[1]Radiology, University of Pennsylvania, Philadelphia, Pennsylvania, United States, [2]Otolaryngology–Head & Neck Surgery, Johns Hopkins University, Baltimore, Maryland, United States

INTRODUCTION: Chronic obstructive pulmonary disease (COPD) is currently the fourth leading cause of death in the United States and is projected to become the third leading cause of death worldwide by the year 2020. While several factors contribute to the development of COPD, such as occupational exposure and air pollution, tobacco smoking is the major contributing factor to the development and progression of this group of respiratory diseases. Hyperpolarized (HP) ^{3}He diffusion MRI as a non-invasive imaging technique has demonstrated sensitivity to airway and acinar remodeling. In this study, we utilized a murine model of chronic exposure to cigarette smoke to acquire both apparent diffusion coefficient (ADC) and ventilation of HP ^{3}He in the mouse lungs. The goal of this work was to assess the sensitivity of these HP gas MRI techniques to cigarette smoke-induced changes in lung function and structure as a method of early and effective diagnosis of COPD.

METHODS: Male BALB/c mice (3~4 month old; 26±2g) were randomized into three 10-animal cohorts: 1) naïve, 2) control (housed in a sealed box ventilated with forced room air), and 3) smoked (housed in an identically sealed box ventilated with forced smoked air for 6 months). Prior to imaging, animals were anesthetized, intubated with a 1.5-mm endotracheal tube and mechanically ventilated using a custom small-animal MR-compatible ventilator with a delivery accuracy of ±100μL/breath. Blood oxygenation, heart rate, and temperature were continuously monitored. The mice received a mixture of ^{4}He:O_2 (4:1), V_T = 1 ml/100g body weight; 110 BPM; I:E=1:2; FIO_2=20%. Imaging was performed with centric phase-encoding in a 50-cm bore 4.7-T MRI scanner (Varian Inc) equipped with a 12-cm, 25-G/cm gradients and a 1.5"-ID quadrature 8-leg birdcage body coil (Stark Contrast). Three coronal slices were acquired with the following imaging parameters: FOV=3×3cm^2, ST=5mm, MS=64×64, α=4~5°, TR=6.6ms, and TE=4ms. For ADC imaging, a diffusion-weighted gradient echo imaging pulse sequence was used with diffusion-sensitizing gradients along the phase-encoding (L–R) direction with the following timing parameters: Δ=1ms, δ=200μs, and τ=180μs according to the naming convention of [1]. Mice were ventilated with ten identical breaths of HP ^{3}He:O_2 (4:1) at the designated tidal volume followed by a 1.5-sec breath-hold during which three coronal slices (covering the entire lung) were acquired with one of following *b*-values = 0.00, 3.73, 0, –3.73 s/cm^2. After 30 ^{4}He:O_2 breaths, the procedure was repeated with another *b*-value from the series. These diffusion-weighted images were then combined to yield the ADC map of the imaged slice according to a double-acquisition analysis scheme described earlier [2]. For fractional ventilation imaging, images were acquired with the same positioning using a standard gradient-echo sequence with TR/TE=5.8/3.6ms. Analysis was performed according to the procedure described earlier [3].

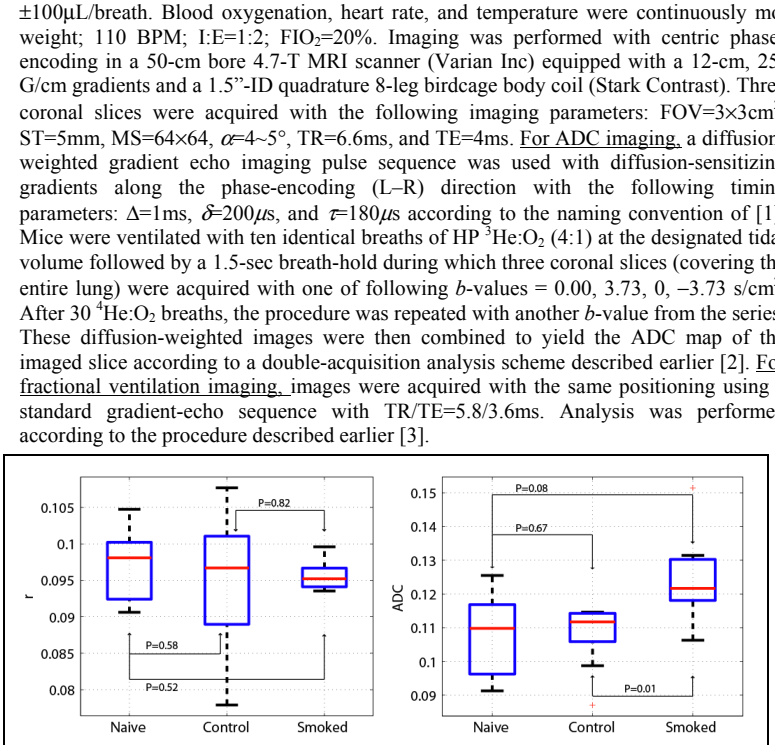

Figure 1. Sample lung parameter maps from a member of each cohort: (a) the naïve group, (b) the control group and (c) the smoked group. Within each image set, posterior (left), middle (middle) and anterior (right) ventilation maps appear at the top and the corresponding ADC maps appear at the bottom. At the right side of the figure, histograms across all three slices are shown.

Figure 2. Pairwise t-test of mean ADC and ventilation among the 3 cohorts.

RESULTS AND DISCUSSION: Figure 1 shows representative maps of fractional ventilation and ADC, along with the corresponding frequency distribution histograms for one animal from each group. Ventilation measurements were statistically similar among the three cohorts, suggesting that the smoke exposure caused minimal modification of airway lumen. The ADC measurements however demonstrated that the smoked lungs' microstructures were somewhat larger and more heterogeneous than those of the other groups. **Table 1** summarizes the experimental results as whole-lung mean ADC values with standard error of the mean in each group. Threshold analysis allows for better stratification of localized disease foci; the optimal ADC threshold includes ~91% of the ADC distribution in the smoked group, but ~97% in their control/naïve counterparts. **Figure 2** shows the pairwise analysis of variance for group mean ventilation and ADC values in all three cohorts, and the corresponding p-values. The difference in ventilation between healthy (naïve and control) mice and smoked mice was statistically insignificant, whereas a significant difference in ADC between healthy and smoked mice was observed.

Cohort	ADC [cm^2/s]	Population Cutoff	80% Threshold	Anterior	Middle	Posterior
Naïve	0.101 ± 0.004	97.21	0.124	0.108 ± 0.005	0.102 ± 0.004	0.096 ± 0.006
Control	0.104 ± 0.004	96.23	0.130	0.108 ± 0.004	0.111 ± 0.005	0.097 ± 0.006
Smoked	0.120 ± 0.007	91.61	0.145	0.125 ± 0.006	0.122 ± 0.008	0.112 ± 0.006

Table 1. Mean ADC values in three slices, the population with 80% cutoff and the ADC values below 80% cutoff

CONCLUSION: Preliminary results show that regional measurements of ^{3}He ADC, a measure of lung morphology, is sensitive to differences between smoke-exposed mice over a period of 6 months and the healthy controls. Measurements of ventilation are unaffected over this time period, suggesting that this murine model of chronic exposure to cigarette smoke primarily resembles emphysematous changes in human lungs, as opposed to chronic bronchitis disease. ^{3}He ADC is a promising tool for the study of this model and the asymptomatic changes resembling characteristics of the early human disease.

REFERENCES: [1] Yu, J, *et al.* J Magn Res Imag 2007; [2] Emami, K, *et al.* Proc Intl Soc Mag Reson Med 2007; [3] Deninger AJ, *et al.* Magn. Reson. Med 2002.